5 An adhesively-bonded cast glass system for the Crystal Houses façade

Design principles and experimental validation of an adhesively bonded system utilizing cast glass components[38].

Chapter 4 provided an overview of the three structural systems utilizing cast glass components in architecture, including a brief overview of the work presented in this dissertation. This chapter presents the design principles and experimental work for the first of the two systems explored in this work: a transparent, adhesively-bonded glass block system designed for self-supporting envelopes. The proposed system was developed for the *Crystal Houses* façade in Amsterdam, designed by *MVRDV* Architects. The system is exclusively constructed by solid cast glass blocks, bonded with *DELO Photobond 4468*, a colourless, UV-curing adhesive. This allows for a system of an increased transparency, sparing the necessity of an opaque substructure. In contrast with previous realized projects, solid soda-lime glass blocks are used rather than borosilicate ones.

Initially, several architectural prototypes, comprising glass elements of different tolerance ranges, are built to evaluate the visual performance and the thickness of the adhesive that allows for an even spread. The prototypes indicate that a homogeneous bond thicker than 0.3 mm cannot be obtained by the selected adhesive due to the latter's flow properties and low viscosity. Based on the adhesive's optimum application thickness, it is determined that the glass blocks' top and bottom surfaces should be flat within 0.25 mm for guaranteeing an even adhesive layer of the highest strength.

---

38   This chapter has been published as Oikonomopoulou F., Veer F.A., Nijsse R., Baardolf K. *A completely transparent, adhesively bonded soda-lime glass block masonry system*. Journal of Façade Design and Engineering 2014. (Oikonomopoulou et al. 2015b)

TOC

The structural verification of the system is demonstrated by physical testing of prototypes in compression, 4-point bending, hard-body impact and thermal shock. Compressive tests on individual blocks highlight the need for proper detailing and uniform load distribution of the system. Compressive tests on columns made of adhesively bonded glass blocks further confirm that strict size tolerances are essential for maximizing the load-bearing capacity of the system: specimens with larger size deviations fail in considerably lower stress values than specimens with smaller size deviations. Furthermore, series of 4-point bending tests on adhesively bonded glass beams demonstrate that the chosen adhesive enables the glass brick wall to behave monolithically under such loading when the adhesive is applied in a constant layer of the optimum thickness.

Overall, the results show that the adhesively bonded glass block structure can provide the required structural performance, but only if strict tolerances are met in the geometry of the glass blocks so that the chosen adhesive can be evenly spread in a constant thickness.

Credits

4-point bending tests conducted in collaboration with
— Telesilla Bristogianni,
Faculty of Civil Engineering & Geosciences, TU Delft

Technical support and assistance
— Kees Baardolf - *prototype construction & preparation of test set-ups,*
Stevin II Laboratory, Faculty of Civil Engineering & Geosciences, TU Delft
— Marco & Ronald van de Poppe – *assistance in construction of wall mock-ups*

Test facilities
— *Compression tests, Impact & Vandalism Test*
Stevin II Laboratory,
Faculty of Civil Engineering & Geosciences, TU Delft
— *4 point-bending tests*
Materials Laboratory,
Faculty of Mechanical, Maritime & Materials Engineering

Research Supervisors
— Rob Nijsse,
Faculty of Civil Engineering & Geosciences, TU Delft
— Fred A. Veer,
Faculty of Architecture & the Built Environment, TU Delft

Architectural Design
— MVRDV

Co-Architect
— Gietermans & Van Dijk

Glass brick manufacturer
— Poesia

Adhesive Consultant
— Siko B.V. - Rob Janssen

5.1 Introduction

This chapter focuses on the research, development and experimental validation of an adhesively-bonded solid glass block self-supporting system. The proposed system has been developed for the *Crystal Houses* façade in Amsterdam, designed by *MVRDV* and successfully completed in 2016. The architectural concept behind the façade is the creation of an accurate yet completely transparent reproduction of the previous 19th century elevation of the building of 10m x 12m in dimensions. In turn, the façade is exclusively constructed by solid glass blocks, bonded by a colourless, stiff adhesive. Soda-lime glass is opted for the fabrication of the glass blocks due to cost reasons. Given the insufficient, if any, guidelines on such an adhesive application, research is conducted on choosing a suitable adhesive for the bonding of the blocks that allows for the desired visual and structural performance and for a relatively quick construction. Several architectural prototypes are built to evaluate the visual performance and to investigate the optimum thickness range of the adhesive, and correspondingly to determine the allowable size deviations of the glass blocks. The structural performance of the adhesively bonded glass block assembly is evaluated through a series of experimental tests of real size prototypes. In specific, physical prototypes are tested in compression, 4-point bending, hard-body impact and against thermal shock. The experimental work and the results are discussed in sections 5.5 and 5.6.

5.2 The case study

The novel glass masonry façade has been designed and engineered to replace the brick façade of a former townhouse in Amsterdam, aiming to preserve the city's traditional architectural style and historical ensemble. Designed by the *MVRDV* architectural studio (www.mvrdv.nl), the innovative façade follows the original 19th century elevation down to the layering of the bricks and the details of the window frames, but is stretched vertically to comply with updated zoning laws and allow for increased interior space (MVRDV Architects 2016) (Fig. 5.1). Based on the brick modules of the original masonry façade, the 10 m x 12 m elevation consists of more than 6500 solid glass bricks, each 210(±1) mm thick by 65(±0.25) mm high by 105/157.5/210 (±0.25 mm) wide, reinterpreting the traditional brickwork and the

characteristic architraves above the openings; while massive cast glass elements reproduce the classic timber door and window frames. As it ascends, terracotta bricks intermingle with glass ones, gradually transforming the glass elevation to the traditional brick façade of the upper floor (Fig. 5.2). The end result is a building that will stand out, and at the same time will naturally blend into the urban fabric of the historic street.
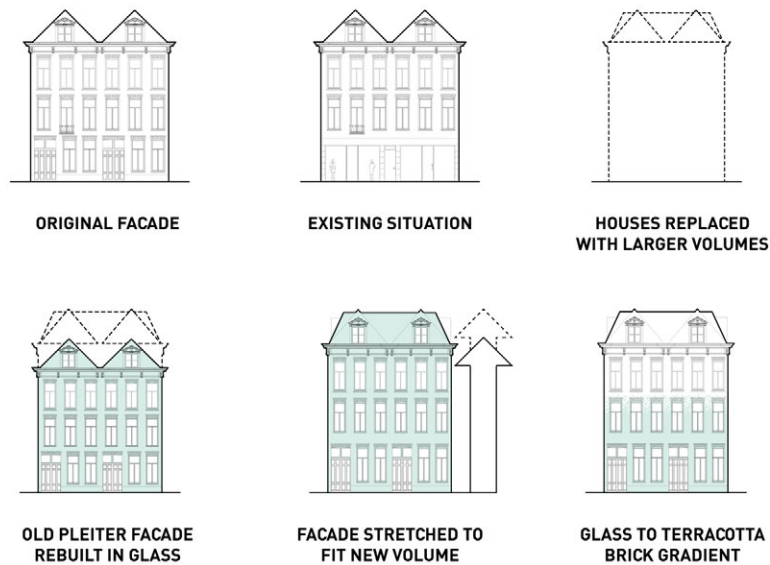

ORIGINAL FACADE **EXISTING SITUATION** **HOUSES REPLACED WITH LARGER VOLUMES**

OLD PLEITER FACADE REBUILT IN GLASS **FACADE STRETCHED TO FIT NEW VOLUME** **GLASS TO TERRACOTTA BRICK GRADIENT**

FIG. 5.1 Illustration by *MVRDV* of the concept behind the *Crystal Houses* façade.

The architects' desire for unimpeded transparency excluded the use of a metal substructure, rendering the choice for an entirely self-supporting glass brick system as a necessary and so far unique solution. In specific, the lower 10 m of the facade comprise mainly cast glass solid blocks. At the highest part of the elevation, the glass blocks intermix with conventional terracotta bricks in a limited zone until the first array of solely clay bricks appears (Fig. 5.2). Above this array, a steel beam covered with terracotta bricks is placed to support the upper, traditional brick facade. The beam is connected to the slab of the second floor allowing for the independent construction of the 10 m high glass block wall. From that point up a conventional brick facade with cavity is constructed (Fig. 5.2).

FIG. 5.2 Left: 3D visualization of the *Crystal Houses* façade by *MVRDV* Architects. Right: The realized façade.

In principle, a bearing wall of the aforementioned size comprising exclusively solid glass bricks is feasible owing to the compressive strength of glass (stated between 400-600 MPa for uniaxial loading by (Fink 2000) and 300-420 MPa by (Granta Design Limited 2015) and the considerable cross-section of the solid glass bricks (210 mm) that allow the façade to carry its own weight and have an enhanced buckling resistance[39]. The lateral stability of the façade is guaranteed by 4 buttresses, each 5.5. m tall, erected towards the interior by interlaced glass bricks, resulting in a continuous relief glass envelope of increased rigidity (Fig. 5.3). Due to the higher density of glass compared to masonry, the glass facade, weighs approximately 25% more than a standard masonry facade of the same dimensions. This 25% difference of dead load necessitates a heavier foundation.

Besides the use of glass bricks, the main difference between the old and new masonry system is that the glass wall's thickness is covered by the width of one brick

---

[39] In comparison, a wall of the same dimensions comprising hollow glass blocks would require a supporting sub-structure. Their reduced thickness results in internal buckling or stress concentrations that in turn lead to a relatively low stated resistance in compressive load (defined as low as 6 MPa in ISO 21690:2006 by (International Organization for Standardization 2006)).

(210 ±0.25 mm) instead of two, as is the case in normal masonry (Fig. 5.4). This was specifically chosen to eliminate unnecessary joints that can affect both the structural and optical performance/clarity of the glass structure. Accordingly, to reproduce the isodomic brick modulus of the historic facade, all glass blocks present the same width (210 ±0.25 mm) and height (65 ±0.25 mm) but are cast in 3 different length sizes (105, 157.5 and 210 ±0.25 mm).
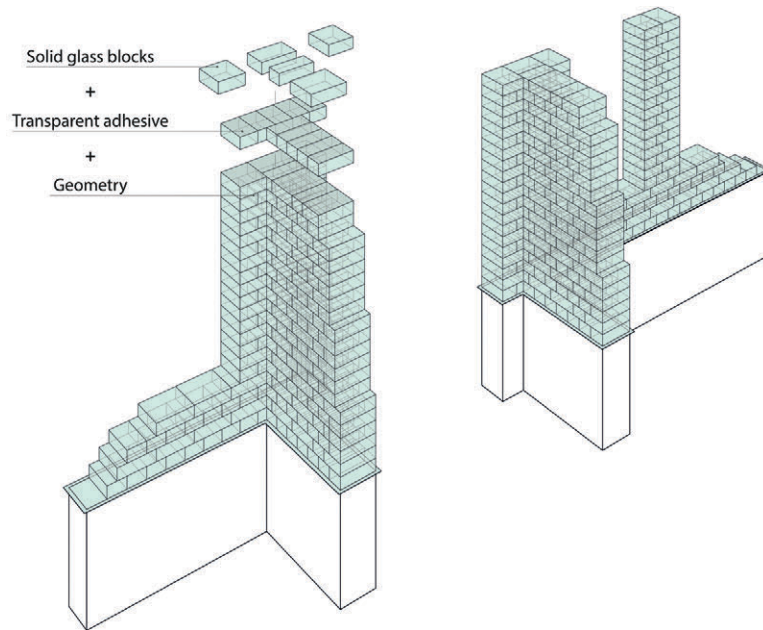

FIG. 5.3 Schematic illustration of the applied buttress system.
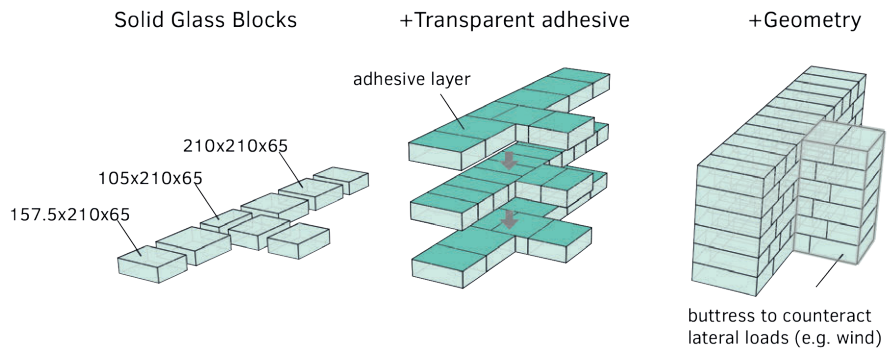

FIG. 5.4 Basic structural scheme of the proposed system

TOC

5.3 Methodology

The limited realized examples of self-supporting structures out of solid glass blocks and the lack of standardized structural specifications and building guidelines for such an adhesive application necessitated an holistic research on the materialization and engineering of the façade. Hence, based on the specific application, both the choice of glass recipe and adhesive are investigated and argued upon. The validation of the system is done through a series of experiments that aim to explore both the visual and the structural performance. Initially, series of physical prototypes are made to study the visual performance of the system and to develop a bonding method that allows for the even spread of the adhesive and the minimization of defects such as bubbles, air gaps, etc. The visual mock-ups give valuable input on the maximum tolerances allowed for architectural purposes and for achieving an even layer of the adhesive – the corresponding experiments are presented in chapter 5.4.2. Following, several series of full-scale prototypes are made and are experimentally tested in compression, 4-point bending, hard-body impact and thermal shock in order to derive the mechanical properties and evaluate the safety of the developed adhesively bonded glass block assembly.

5.4 Materials

In this section the choice of adhesive and glass type as well as the manufacturing process of the glass blocks are discussed and analysed.

5.4.1 Selection of Adhesive

The architectural prerequisite was to obtain a completely transparent and at the same time structurally feasible solution. To meet this requirement, a combination of solid glass blocks and colourless adhesive was chosen for the construction of the glass masonry wall. The mechanical properties of the adhesive are equally critical to the ones of the glass bricks for the developed system; it is their interaction as one structural unit that determines the structural capacity and properties of

the assembly. The most favourable structural performance is obtained when the adhesive and glass bricks fully cooperate and the masonry wall behaves as a single rigid unit under loading, resulting in a homogeneous load distribution. More specifically the adhesive should:

— be completely transparent and colourless and not discolour when exposed to sunlight
— present good short and long term compressive behaviour
— establish high bond strength with glass
— result in a monolithic masonry wall
— provide a rigid structure
— present good resistance to weathering and good aging behaviour
— allow for fast, easy and safe construction
— have no emissions of noxious or poisonous chemicals during processing and curing

An adhesive that meets all the above demands is *DELO Photobond (DP) 4468*, a colourless, one-component, UV-curing acrylate, designed for high force transduction in glass/glass and glass/metal bonds (Delo Industrial Adhesives 2014). Adhesives of the *Delo Photobond* family have already been applied for the bonding of all–glass structures, e.g. in the frames of the glass shell of the *Leibniz Institute for Solid State and Materials Research* (Delo Industrial Adhesives 2011; Weller et al. 2012; Weller et al. 2010b, a).

TABLE 5.1 Indicative properties of *Delo Photobond 4468* according to (Delo Industrial Adhesives 2014)

Property	Unit	Delo 4468
Viscosity	mPas (at 23 °C)	7000
Density	g/cm³	1.0
Young's modulus	N/mm²	250
Glass-glass compression shear strength	N/mm²	22
Tensile strength	N/mm²	14
Elongation at tear	%	200
Glass transition temperature	°C	74
Shrinkage	Vol%	9
Index of refraction	-	1.5
Water absorption	weight %	0.9
Creep resistance CTI	-	600M
Shore hardness A	-	83
Shore hardness D	-	45

The selected adhesive is optimized for high force transduction in glass-to-glass and glass-to-metal bonds and presents high shear stiffness, good short and long term compressive behaviour and long lifetime due to high humidity resistance (Delo Industrial Adhesives 2014). Visually, besides being colourless, it has a similar refractive index to glass and does not discolour when exposed to sunlight. Another important feature is its photo-catalytic curing, allowing for fast construction: The adhesive can be fully cured in a minimum of 40 seconds using 60 mW/cm^2 UVA intensity (Delo Industrial Adhesives 2014). After curing, it obtains its full structural capacity and becomes moisture- and water- resistant. The cured product is normally used in a temperature range of -40 °C to +120 °C. The properties of *DP 4468* adhesive are listed in Table 5.1.

## 5.4.2 Defining the optimum thickness range of the adhesive

There are no clear guidelines from the adhesive manufacturer on the recommended application thickness of *DELO Photobond 4468*. Moreover, there is a not yet a generally approved theory concerning the effect of adhesive thickness in the strength of the bond. Although the classical elastic analyses predict that the strength increases with the adhesive thickness, experimental results show the opposite (da Silva et al. 2006). Research by (Grant et al. 2009), (da Silva et al. 2006), and (Crocombe 1989) suggest different reasons[40] why a thicker bond layer provides a decreased joint strength. Based on experimental work by (Riewoldt 2014), Fig. 5.5 exhibits how a comparatively thicker layer can negatively influence a rigid (i.e. epoxy or acrylate) adhesive's bond strength and subsequently the structural performance of the entire system. In practice, (Wurm 2007) mentions that acrylates present their highest strength in an application thickness between 0.1 mm and 0.5 mm, whereas (Puller,Sobek 2008) suggest an optimum thickness of 0.2 mm for a glass to metal bond with *DELO Photobond 4468*.

Prior and parallel to structural testing, several architectural mock-ups of the masonry wall were built to study the visual performance of the system and determine the maximum allowable thickness of the adhesive -and correspondingly the minimum acceptable size tolerances of the blocks- for aesthetic purposes. Initial research

---

[40] (Crocombe 1989) suggests that thicker single-lap joints have a lower strength considering the plasticity of the adhesive, whereas (da Silva et al. 2006) found that interface stresses are higher for thicker bondlines. (Grant et al. 2009) suggests that as the bondline thickness of a T joint increases, there is an increase in the bending stress since the bending moment increases, reducing the strength of the joint.

TOC

indicated that due to the medium viscosity of the selected adhesive (7000 mPa·s at 23°C, measured by *Brookfield* viscometer (Delo Industrial Adhesives 2014)), the vertical joints of the blocks cannot be homogeneously bonded: the adhesive would flow downwards before it could be cured. Therefore, it was determined that only the horizontal surfaces of the glass blocks would be bonded; the vertical ones are left dry, allowing as well for thermal expansion.
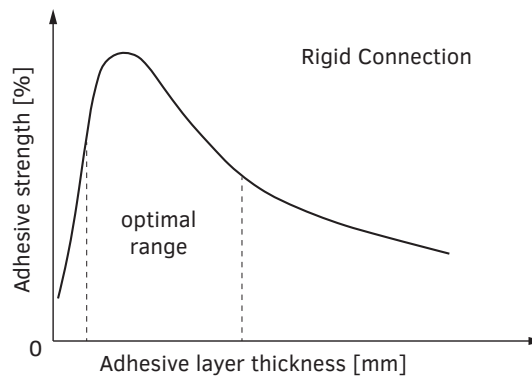
FIG. 5.5 Schematic illustration of the relation between a stiff adhesive's strength and thickness by(Riewoldt 2014; den Ouden 2009; Wurm 2007).

Next, 3 successive wall mock-ups (Fig. 5.7) were made comprising glass elements with a different tolerance range. Multiple trials suggested that a consistent, even adhesive distribution occurs when the adhesive is spread in an X pattern on the bonding surface – this allows any bubbles to be pushed out of the adhesive layer prior to its curing. The findings from the visual prototypes are summarized in Table 5.2. It can be derived that larger tolerances lead firstly to significant offsets in the height and width of the facade, secondly to open joints between adjacent blocks and thirdly, and most importantly, to an uneven spread of the adhesive (Fig. 5.6) that can greatly affect the structural performance of the wall. Besides compromising the visual result, inconsistent bonding introduces weaker structural zones. Especially voids against the glass substrate in stiff adhesives can cause major stress concentrations (O' Regan 2014). The wall prototypes pointed out that a homogeneous bond thicker than 0.3 mm cannot be obtained due to the adhesive's flow properties and medium viscosity. Based on the adhesive's optimum application thickness, it was determined that the glass blocks' top and bottom surfaces should be flat within 0.25 mm for guaranteeing an even adhesive layer of the highest strength. Any accumulated deviation larger than the required 0.2-0.3 mm thickness of the adhesive could lead to uneven and improper bonding.

TOC

FIG. 5.6 Common flaws occurring in the adhesive layer: air gaps, capillary action and dendritic patterns.

Based on the findings, a fourth mock-up was constructed with the desired tolerance on the blocks. In this mock-up, the construction of the buttress was also tested and an improved bonding method was employed: Customized *PURE*® (self-reinforced polypropylene) forms are employed for the distribution of the adhesive in an X pattern, controlling its amount, flow and spread. Once the adhesive is evenly spread, the brick is held in position and under constant (manual) pressure and is exposed to low intensity UV-light for 5 s. This pre-curing step was introduced for practical reasons: the partial curing stabilizes the glass brick to its final position while still allowing the wiping-off of any adhesive overflow. After cleaning, the adhesive is further cured by low and medium intensity UV-radiation, in the range of 20-60 mW/cm^2, for a period of 60 - 180 s, depending on brick size. The final result can be seen in Fig. 5.8.

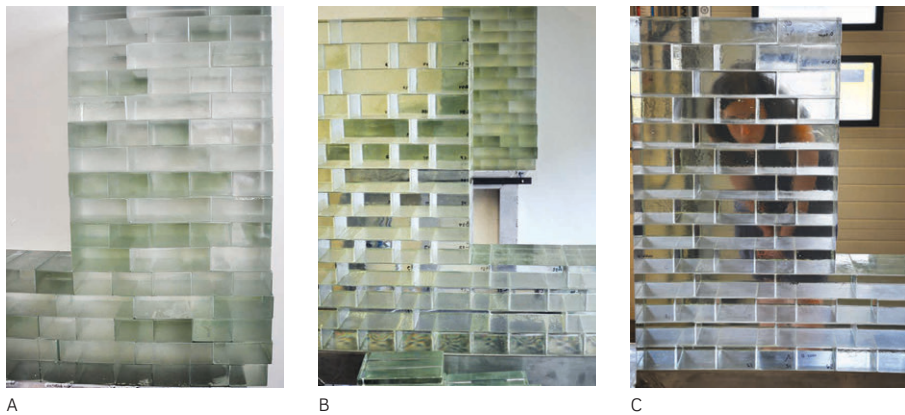A   B   C

FIG. 5.7 Photographs of the three mock-ups. Mock-up A was made with higher tolerances. As a result there were significant offsets in both height and width, as well as open joints between blocks. Mock-up B was made with blocks of higher accuracy that prevented a substantial offset in height. Still, any uneveness up to ±0.5 mm in flatness resulted to cavities and bubbles in the bond area. In mock-up C all blocks meet the ± 0.25 mm tolerance, resulting in an even spread of the adhesive and thus, in homogeneous bonding and satisfactory visual result without any cavities and bubbles of substantial dimensions.

TOC

TABLE 5.2 Observations from the architectural mock ups

Mock-up	Tolerances				remarks
	rectangularity [mm]	height [mm]	width [mm]	flatness [mm]	
A	±0.5	±0.5	±0.5	±0.5	– The inaccuracy in rectangularity leads to open joints of up to 5 mm. – Considerable offsets in both height and width of the prototype – Inconsistency in bonding surface
B	±0.25	±0.25	±0.25	±0.5	– No offset in height and width of the prototype – Inconsistency in bonding surface: bubbles, gaps, unsatisfactory optical result
C	±0.25	±0.25	±0.25	±0.25	– No offset in height and width of the prototype – Uniform distribution of the adhesive, satisfactory optical result.

FIG. 5.8 The final (4th) wall mock-up which includes the buttress's construction by interocking glass blocks

5.4.3 Choice of glass

From the previous chapter it can be derived that the adhesive's low to medium viscosity and ideal bond thickness of a quarter of a millimetre combined with glass's elastic nature introduce exceptionally strict tolerances on the size of the individual glass elements. This accuracy, determined to be ±0.25 mm in the height and flatness of the elements is essential for attaining an even, homogeneous spread of the adhesive, required not only for the most favourable structural capacity, but also for a visual result of maximized transparency. An inconsistent spread of the adhesive can result in visible gaps and bubbles. But most importantly, considering that the joints between adjacent blocks have virtually zero thickness, even a tolerance of 0.5 mm per block could result in a sizeable offset in the height or width of the entire construction.

Cast glass blocks with such strict tolerances in size and flatness have never been produced before. In projects where a metal substructure is employed, sealant joints considerably thicker can be accommodated, which in turn can compensate for substantially coarser tolerances. The sole comparable structure to the one examined here is the *Atocha Memorial*. However, in that case, the overall cylindrical shell geometry contributes greatly to the structure's rigidity, allowing for a tolerance range of ±1 mm (Christoph, Knut 2008) in the size of the blocks, without compromising the structural capacity. This is 4 times more than the tolerance allowed in the presented adhesively-bonded system. The solid glass bricks, used in the *Atocha Memorial*, utilized borosilicate glass and precision press moulds for obtaining highly accurate units (Schober et al. 2007). Borosilicate glass was favoured over soda-lime glass owing to its comparably lower thermal expansion coefficient [$3.2–4 \times 10^{-6}$/K] over soda-lime glass [$9.1–9.5 \times 10^{-6}$/K] (Granta Design Limited 2015). This, in turn, results in considerably less natural shrinkage during cooling and accordingly to a cast element of higher dimensional accuracy. A high precision press mould further confines the cast element to the desired dimensions, by pressing the molten glass during the initial, rapid cooling stage. With this method the desired ±1.0 mm (Goppert et al. 2008) size tolerance was achieved for the cast glass blocks without any machine processing.

Nonetheless, in the given case study, the 10 m x 12 m dimensions of the façade and its flat geometry necessitate an increased masonry strength and consequently require the optimum thickness of the adhesive. The required ±0.25 mm tolerance would necessitate the mechanical post-processing of the blocks' horizontal (bonding) surfaces, even for borosilicate glass. Consequently, to avoid an unnecessary increase in manufacturing costs, soda-lime glass and open precision moulds were opted for the final fabrication of the glass blocks.

Soda-lime is the least expensive form of glass (Corning Museum of Glass 2011d) and requires a significantly lower working temperature than borosilicate. As a drawback, due to the higher thermal expansion coefficient of soda-lime a considerably longer annealing -and manufacturing- time of the components is needed. For example, the borosilicate glass blocks of 70 mm x 200 mm x 300 mm in dimensions and 8.4 kg weight (shown in Fig. 5.9), used in the *Atocha Memorial*, required a total annealing time of circa 20 h (Goppert et al. 2008). Whereas, the comparatively smaller soda-lime glass bricks of 65 mmx 210 mm x 210 mm in dimensions and 7.2 kg weight used in this project, required 36-38 h of annealing time respectively (Fig. 5.10). High precision open moulds were preferred over press moulds, since the use of the latter was considered an expensive and unnecessary solution in view of the inevitable post-processing. The final fabrication method of the glass blocks is described in detail in Section 6.2.1 of the following chapter. An overview of the technical specifications of the soda-lime glass used is given in Table 5.3.

FIG. 5.9 Left: the 300 x 200 x 70 mm borosilicate glass block of the *Atocha Memorial* made by press mould. Centre: a 210 x 105 x 65 mm soda-lime glass block of the *Crystal Houses* prior to post-processing. Right: a 210 x 105 x 65 mm soda-lime glass block of the *Crystal Houses* after post-processing.

TABLE 5.3 Technical specifications of the soda-lime cast glass blocks as provided by *Poesia*

Average compression resistance	397 N/mm²
Thermal conductivity	0,974± 0,036 W (m K)
Linear Thermal dilatation coefficient	10.2 - 10.6 (10^{-6} °C^{-1})
Mohs hardness	3
Fire resistance	REI 60 by standard pose with cement mortar

To ensure that the higher expansion coefficient of soda-lime glass will not cause excessive thermal stresses on the façade, a simulation of the expected thermal loads in a yearly cycle was performed by an external company specializing in building physics. Based on the optical transmittance data provided by *TU Delft* for the solar gain (see Fig. 5.11), the orientation of the specific location, the height of the surrounding buildings and the assumption of a constant heating load in

winter and cooling load in summer from the indoors air-conditioning, heat and light transmittance of the wall were simulated. The results indicated acceptable thermal strains (less than 14.3×10^{-3}) for the soda-lime cast glass even under the most extreme weather conditions for Amsterdam.

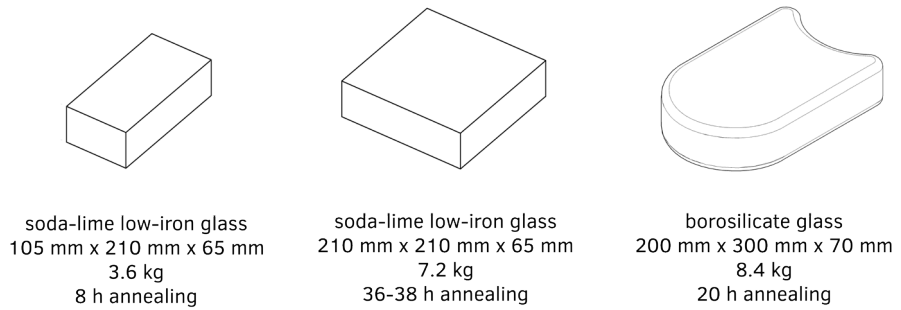| soda-lime low-iron glass	soda-lime low-iron glass	borosilicate glass
105 mm x 210 mm x 65 mm	210 mm x 210 mm x 65 mm	200 mm x 300 mm x 70 mm
3.6 kg	7.2 kg	8.4 kg
8 h annealing	36-38 h annealing	20 h annealing

FIG. 5.10 Size and annealing time of the *Crystal Houses* blocks (left and centre) and of the *Atocha Memorial* block (right).
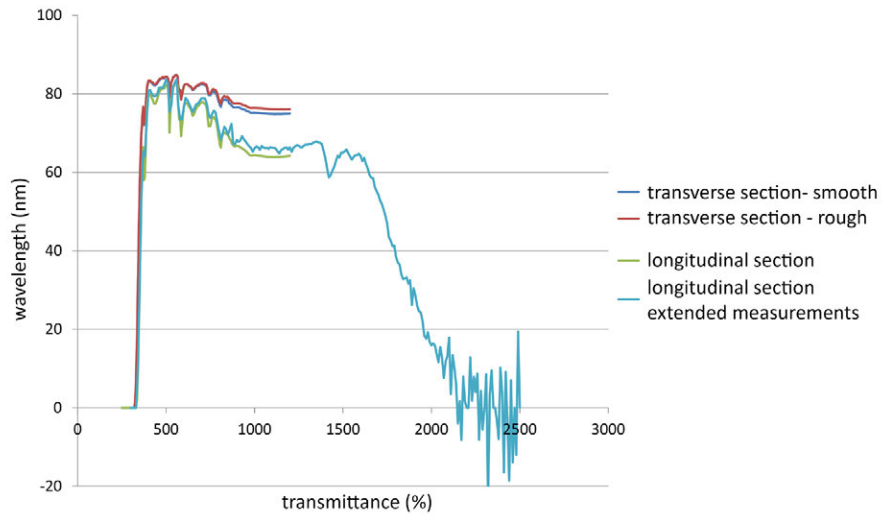

FIG. 5.11 Optical transmittance data of a standard *Poesia* brick by (Tijssen 2014).

5.5 Experimental

5.5.1 Test specimens

The novelty of the developed glass system came with a lack of standardized strength data and building guidelines on both solid glass blocks and chosen adhesive. Accordingly, in order to determine the structural behaviour of the glass-adhesive system and validate the proposed tolerance specifications of the bricks as well as the adhesive's application method, a wide range of structural experiments had to be carried out. In summary, the following experiments have been conducted over the course of 18 months:

— Compression of single blocks
— Compression of glass pillars out of adhesively bonded glass blocks
— 4-point bending tests on glass beams out of adhesively bonded glass blocks
— 4-point bending test of a glass architrave out of adhesively bonded glass blocks
— hard body impact and vandalism test of an adhesively bonded glass wall
— thermal shock of individual glass blocks

Fig. 5.12 provides an illustrated overview of the tests and the dimensions, composition and number of prototypes per test. All prototypes have been made with soda-lime solid glass blocks cast by *Poesia* company in Italy. The glass block assemblies are bonded together with *Delo Photobond 4468* (DP 4468), except if stated otherwise. Five different glass block sizes have been used in the prototypes – the different sizes are presented in Table 5.4. At the early stages of this research, prototypes have been made with standard *Poesia* bricks, namely N_s and N_L blocks. These blocks are included in the standard production of *Poesia* and had been readily-available for manufacturing prototypes for experimental work. These first prototypes and corresponding experiments have been valuable for validating the necessity of the required flatness tolerance of ± 0.25 mm of the blocks, essential for achieving the desired structural behaviour of the adhesively bonded solid glass block system. The custom-made blocks of ± 0.25 mm precision in size and flatness, namely S, M and L, had been manufactured several months later by *Poesia*, and after exploring multiple variables through the aid of visual prototypes, described in chapter 5.4.2. In addition, the final custom-made blocks (S, M and L) follow the general dimensions desired by *MVRDV Architects* so that the block modulus matches the one of the previous, 19th century elevation of the building.

For the ease of the reader, the extensive experimental research is not presented in chronological order, but instead, in the most reasonable order. Some initial experiments comprising different adhesives or block configurations have been excluded on purpose, as they were considered insufficient for deriving statistical data.

Test name	Specimen composition	Number of specimens
Compression test - individual blocks specimens	A_L, 65 mm, 210 mm; A_M, 65 mm, 157.5 mm; A_S, 65 mm, 105 mm. S, M and L blocks (thickness 210 mm)	3 A_L 3 A_M 3 A_S
Compression test - glass pillars specimens	N_L blocks bonded with DP 4468 along the horizontal joints only. N_S blocks bonded with DP 4468 along the horizontal joints only. B_{NL1} 492 mm, 232 mm 106 mm; B_{NL2} 464 mm, 246 mm 106 mm; B_{NS1} & B_{NS2} 484 mm, 116 mm 116 mm	1 B_{NL1} 1 B_{NL2} 2 B_{NS}
4-point bending test - glass beam specimens	C. 300 mm, S, M and L blocks bonded with DP 4468 along their horizontal joints and along the bottom-layer's vertical joints. 195 mm, 210 mm. 1000 mm, 1155 mm	4
4-point bending test architrave specimen	280 mm. customized tapered blocks bonded along the vertical joints with DP 4468. DP 4494 has been applied in few locations were the joint gaps were above 0.3 mm thick. The horizontal joints are left open. 230 mm, 330 mm, 210 mm. 1800 mm	1
Impact & vandalism test - wall specimen	N_L blocks bonded with DP 4468 along the horizontal joints only. 580 mm, 53 mm. 1230 mm	1
Thermal shock specimens	F_1, F_2, F_3, F_4. N_L blocks tested in thermal shocks by different types of water immersion after they are pre-heated for 4 hours to 60 °C and 80 °C degrees.	60 °C: 2 F_1 2 F_2 2 F_3 2 F_4 / 80 °C: 2 F_1 2 F_2 2 F_3 2 F_4

FIG. 5.12 Overview of tests and of the various dimensions, composition and number of specimens.

TABLE 5.4 Type of blocks used for the manufacturing of the prototypes

Brick type	Dimensions	Size Tolerances	Material
N_S	121 x 116 x 53 mm	± 0.5 mm	Soda-lime glass
N_L	246 x 116 x 53 mm		
S	105 x 105 x 65 mm	± 0.25 mm	Soda-lime, low-iron glass
M	157.5 x 105 x 65 mm		
L	210 x 105 x 65 mm		

5.5.2 Set-up of compression tests on single blocks

To investigate the compression strength of the glass blocks, three series of soda-lime blocks of the different custom-made sizes (S, M and L) have been tested in a displacement-controlled hydraulic compression machine of 3 MN maximum load capacity. In the first two series of tests, the blocks have been placed directly on the machine's metal surface; in the third series, two 18 mm thick plywood sheets have been inserted between each glass block and the steel surfaces of the testing machine (Fig. 5.13). For safety reasons, all specimens were wrapped in several layers of clear PET plastic foil and were placed in a safety steel cage with polycarbonate windows.
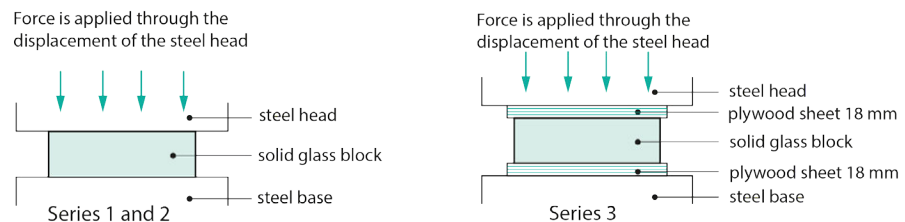

FIG. 5.13 Set-ups of the compression tests on single glass blocks.

5.5.3 Set-up of compression tests on glass pillars out of adhesively bonded glass blocks

4 glass pillars have been tested in a force-controlled hydraulic compression machine, to investigate the compression strength of the glass block-adhesive system. The columns have been constructed of standard N_L *Poesia* blocks (specimens B_{NL1} and

B_{NL2}) and N_S blocks (specimens B_{NS1-2}), adhesively bonded along their horizontal joints only. Three different configurations have been formed (Fig. 5.14), to study how the strength is affected. B_{NL1} and B_{NL2} columns were adhesively bonded across the largest faces of the N_L bricks. These faces present a convex plane of approximately 0.5 mm at the centre. Thus, the bonding layer is of a variable thickness: it is thinner at the edges and thicker in the middle of the brick. Specimens B_{NS1} and B_{NS2} use a different configuration and a different block size (N_S): the glass blocks are bonded across their shorter and much more even surfaces, resulting to a consistent adhesive layer thickness of approx. 0.2 – 0.3 mm.

Two 18 mm thick plywood sheets have been placed at the top and the bottom surface of each pillar to prevent direct contact between the glass elements and the steel surface of the machine. During the experiment, a transparent plastic box was placed around the column as a safety precaution.
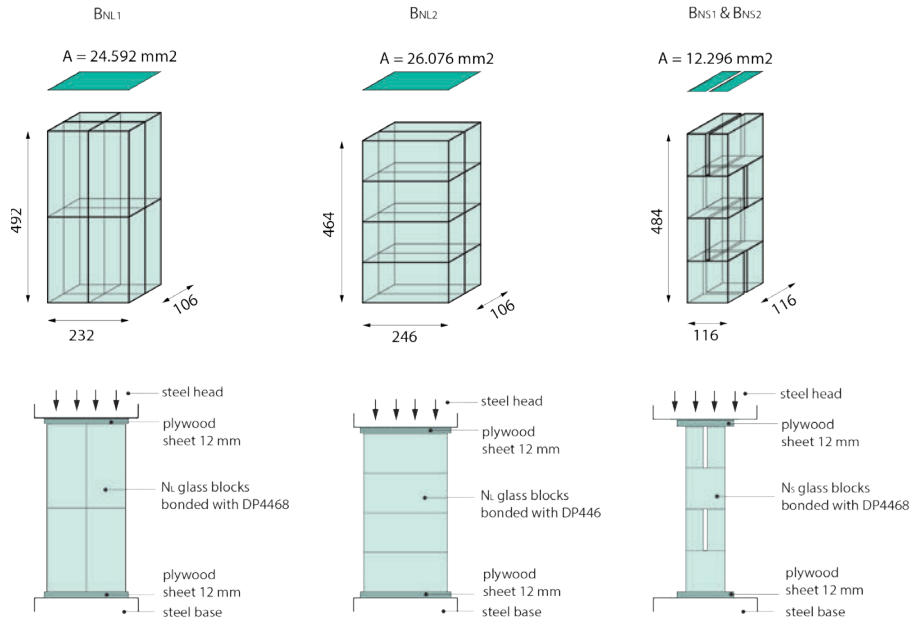

FIG. 5.14 Dimensions and experimental set-up of the glass pillars.

5.5.4 Set-up of 4-point bending tests on glass beams out of adhesively bonded glass blocks

To determine the flexural strength of the glass masonry wall, 4 glass beam prototypes were constructed and tested in-plane in 4-point bending until failure. Each specimen was made of 23 solid soda-lime glass bricks, bonded together into a beam configuration by *Delo Photobond 4468*. More in detail, each specimen consists of 3 arrays of glass blocks. The top and bottom arrays comprise each 2 M and 4 L glass blocks, while the middle array consists of 11 S blocks. The dimensions, configuration and experimental set-up of each specimen are illustrated in Fig. 5.16. In the proposed masonry system, the blocks are bonded only along their horizontal faces. Nevertheless, in order to represent more accurately the boundary conditions of the glass masonry wall in the specimens, the blocks forming the bottom array have also been bonded to each other along their vertical faces to achieve a continuous bottom zone. The glass blocks of the upper two arrays have been bonded only along their horizontal surfaces, leaving open vertical joints.

The specimens are tested in in-plane 4-point bending until failure in a *Zwick Z100* displacement-controlled universal testing machine, where the upper steel head moves downwards with a constant displacement rate of 2 mm/min. A specially fabricated steel frame is used for the bottom supports of the experimental set-up (see Fig. 5.15). None of the supports corresponded to a joint (*see* Fig. 5.16). Prior to testing, all specimens were wrapped in several layers of clear PET plastic foil as a safety precaution.
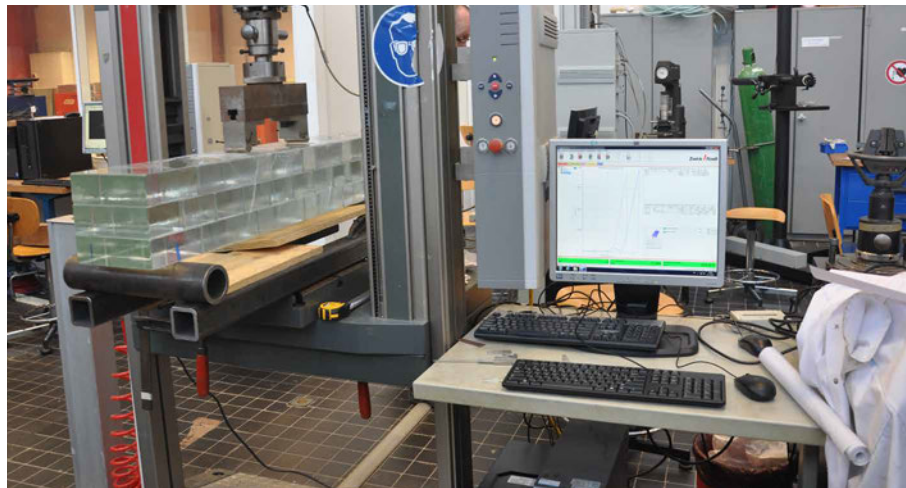

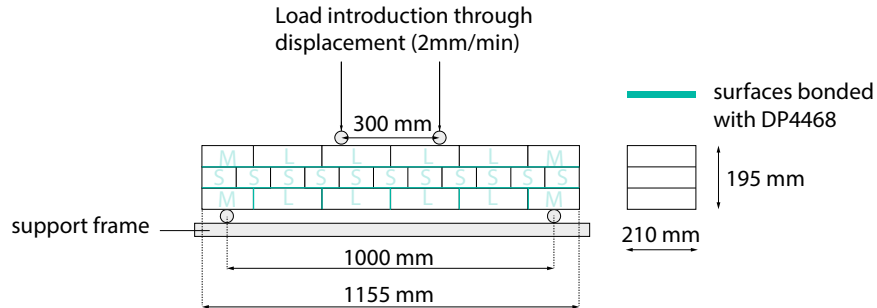FIG. 5.15 Experimental set-up of the 4-point bending tests

FIG. 5.16 Illustration of the 4-point bending experimental set-up

5.5.5 Set-up of 4-point bending test of glass architrave

A glass architrave was also tested in 4-point bending to verify if during installation it can be self-supporting until it is completely bonded to the surrounding wall. The glass arch specimen, consisting of 2 arrays of tapered glass blocks, was constructed from customized solid soda-lime glass blocks cast by *Poesia*: each brick has a different size correspondent to a specific location. The smaller upper blocks are offset 20 mm to create an anaglyph (Fig. 5.18). The dimensions, configuration and experimental set up of the specimen are illustrated in Fig. 5.17. To form the arch, the glass blocks had been bonded together along their vertical surfaces by *DP 4468*. A custom-made rotating steel fixture was employed to assemble the architrave and apply the *DP 4468* horizontally[41]. Due to higher intolerances (greater than 0.3 – 0.4 mm), a thicker but comparably less stiff type of the same adhesive family, *Delo Photobond 4494* (*DP 4494*)*,* was applied in three locations between adjacent blocks[42]; the locations, indicated in Fig. 5.17, where marked before the arch was tested. The properties of *DP 4494* can be found in the Appendix.

---

[41] For a detailed explanation of the architrave's construction method please refer to chapter 6.3.4.

[42] The choice of using an alternative adhesive on some locations to perform this test was due to practical limitations: The blocks for the glass architrave were all of customized size and there were no spares available. Thus, due to time constraints the architrave had to be manufactured with the provided blocks. Since some of the blocks did not meet the required tolerance of ± 0.25 mm and DP 4468 could not fill sufficiently the larger joint on those locations, it was determined to use *DP 4494* instead which is less stiff but can be applied in a thicker layer.

The specimen was tested in in-plane 4-point bending until failure in a *Zwick Z100* displacement-controlled universal testing machine, with a speed of 2 mm/min. A specially fabricated steel frame was used for the bottom supports of the experimental set-up (see Fig. 5.18). The architrave was placed to the testing machine with the aid of a crane. The architrave was loosely supported by ropes from the crane during testing to prevent the falling of big pieces on the floor after failure.
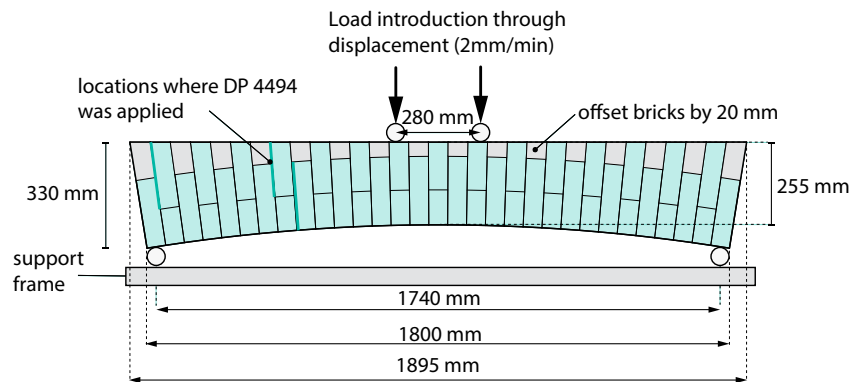

FIG. 5.17 Dimensions and experimental set-up of the glass architrave

FIG. 5.18 4-point bending set-up of the architrave

TOC

Impact and vandalism test set-up

The glass masonry facade could be potentially subject to impact from a variety of causes, such as the accidental impact from bicycles, skateboards, etc. or to the sustained attack with objects such as bottles, bricks, tools, etc. in the case of vandalism. Hence, a rigid body impact test and a vandalism test were performed on an experimental glass wall. The mock-up consisted of 22 N_L blocks, adhesively bonded to form a wall (*see* Fig. 5.19). The glass wall mock-up was mounted into a wooden frame, which was fixed to a rigid concrete wall to simulate the inertia conditions of the glass facade. The specimen was not pre-loaded in compression. Considering the total dimensions of the façade and based on an even dead-load distribution the expected pre-compression of the entire envelope is of less than 0.2 MPa at the lower rows of the façade. This amount of pre-stress in compression is virtually negligible for a glass structure.
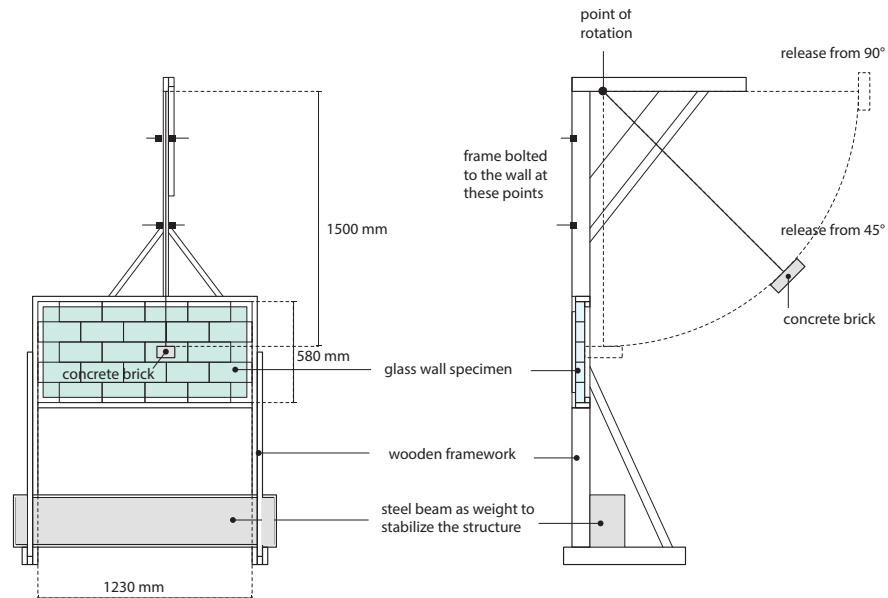
FIG. 5.19 Schematic illustration of the hard body test set-up.

Two different tests were conducted to the specimen:

— a hard body impact test by a solid concrete brick suspended from 45 and 90 degrees angle
— a vandalism test by a 4 Kg sledgehammer

In the hard body impact test, a concrete brick of 65 x 102.5 x 215 mm in dimensions and 3.4 kg in weight was placed in front of the facade, touching the target brick. At that position it was suspended with a hook from a 1.5 m long metal wire, hanging down from a wooden cantilever projecting above the mock-up (see Fig. 5.19 and Fig. 5.20). The concrete brick, attached to the wire, was then swung outwards by a 45 degrees angle and released from there. The test was repeated 2 times from a 45 degrees angle, then another 2 from 90 degrees angle.

Afterwards, a vandalism test was carried out on the same experimental wall using a 4 Kg sledgehammer wielded by the author.
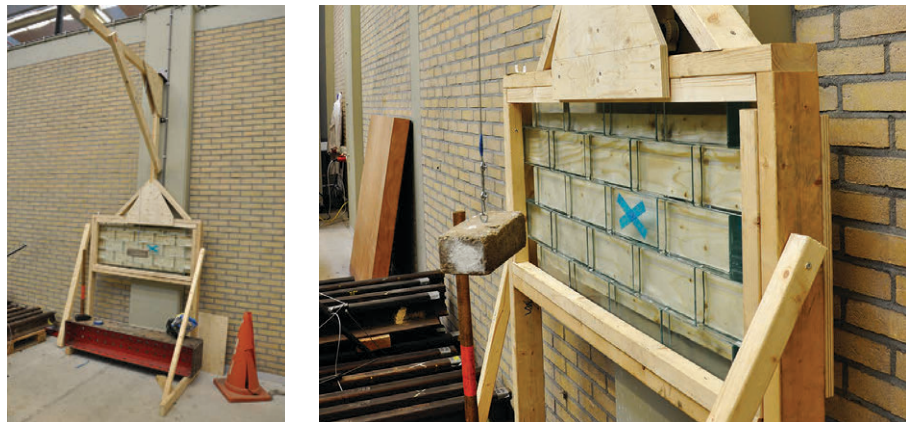

FIG. 5.20 Set-up of the hard body impact and vandalism test

5.5.7 Set-up of thermal shock test on single blocks

On a warm, sunny day the glass blocks can heat up significantly. In the event of rain on the same day, the warmed glass blocks will come into contact with the colder rainwater and a limited thermal shock can occur. The shock intensity is related to the temperature difference between the material and the environment and the rate of heat flow from the glass. In this context, a hot-cold thermal shock is more harmful to glass than a cold-hot thermal shock, because it generates tensile stresses on the rapidly cooled surface. These stresses may be sufficient to activate pre-existing micro-cracks and lead to fracture. Hence, to evaluate the performance of the glass blocks under peak temperature fluctuations, specimens were heated for 4 h in a furnace with a constant temperature of 1) 80°C and 2) 60°C. Following, they were

cooled down by being immediately immersed into water of 20°C for approximately 10 min each. Specimens were:

— half-immersed into water (F_1)
— completely immersed into water (F_2)
— immersed only with one face into the water (F_3)
— splashed on one face (F_4)

Two samples were used per test per temperature. An illustration of the test set-ups is shown in Fig. 5.21.

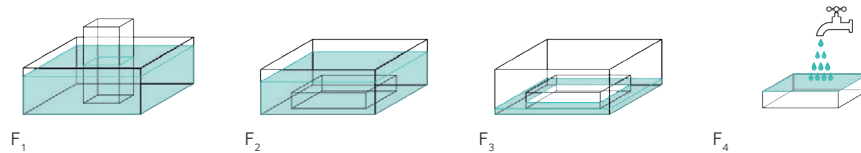F_1 $\qquad$ F_2 $\qquad$ F_3 $\qquad$ F_4

FIG. 5.21 Illustration of the four different thermal shock tests

5.6 Results and Discussion

5.6.1 Compressive tests on single blocks

Table 5.5 summarizes the results of the compressive tests on single blocks. The compressive tests were interrupted when the first cracks were (visibly) observed. In general, the crack patterns in all tested specimens demonstrate the absence of internal residual stresses in the glass blocks, indicating in turn a proper annealing cycle. In specific, no secondary crack branching – an effect of internal residual stress – was observed in any of the specimens, even under high compression loads.

The results of the two first specimens per compression series (A_s, A_M and A_L), where no intermediary was used between the glass blocks and the steel head of the testing

machine, presented obvious cracks in a nominal compressive stress between 20-30 MPa; this is significantly less than the compressive strength value of glass stated in literature[43]. The reduced compressive stress is attributed to the high concentrated contact pressure between the stiff glass blocks and the stiffer steel plates of the compression machine (see Fig. 5.22). Any unevenness or micro-asperity in the contact surface of the two hard materials induces local peak tensile stresses, which, in a brittle material like glass, propagate local cracks[44]. This stresses the importance of properly supporting the glass components along their whole surface and preventing any stress concentration in the supports.

TABLE 5.5 Results of glass blocks' compression tests

Specimen series	Dimensions [mm]	Specimen number	End conditions	Load at first observed crack [kN]	Nominal compressive stress at first observed crack [MPa]
A_S	210x105x65	1	Direct contact with steel	1690[†]	76.6
		2	Direct contact with steel	500	22.7
		3	Wooden intermediary	2977	135
A_M	210x157.5x65	1	Direct contact with steel	999	30.2
		2	Direct contact with steel	870	26.3
		3	Wooden intermediary	>3000*	>90.70
A_L	210x210x65	1	Direct contact with steel	1248	28.3
		2	Direct contact with steel	882	20
		3	Wooden intermediary	> 3000*	>68

* Max. load capacity of the testing machine. No cracks were observed up to the max. load in these specimens.
† At this load multiple cracks were already observed at the specific specimen.

Accordingly, to ensure an even load distribution, in the third specimen of each series, an 18 mm thick plywood plate was used as intermediary on both the top and bottom surface of each glass block (see Fig.5.22). In this series, the smallest block (A_{S3}), presented its first crack at 2980 kN load, a load 5 times higher than the complete dead load of the *Crystal Houses* façade. The block specimens of larger dimensions (A_{M3} and A_{L3}) did not crack until the compressive machine reached its force limit of 3000 kN. This series of experiments emphasizes the importance of designing proper

---

43 Even so, each of the tested S blocks could withstand a load higher than the 40t (392.4 kN) dead load of the designed façade prior to failure.

44 For a more elaborate explanation on the influence of flaws on the strength of glass refer to Chapter 2.6.

connections that ensure an even load distribution to the glass masonry wall. Poor detailing or execution can result in high local stresses that significantly reduce the overall strength of the glass structure. Connections that provide a uniform load distribution will result in considerably higher failure loads.
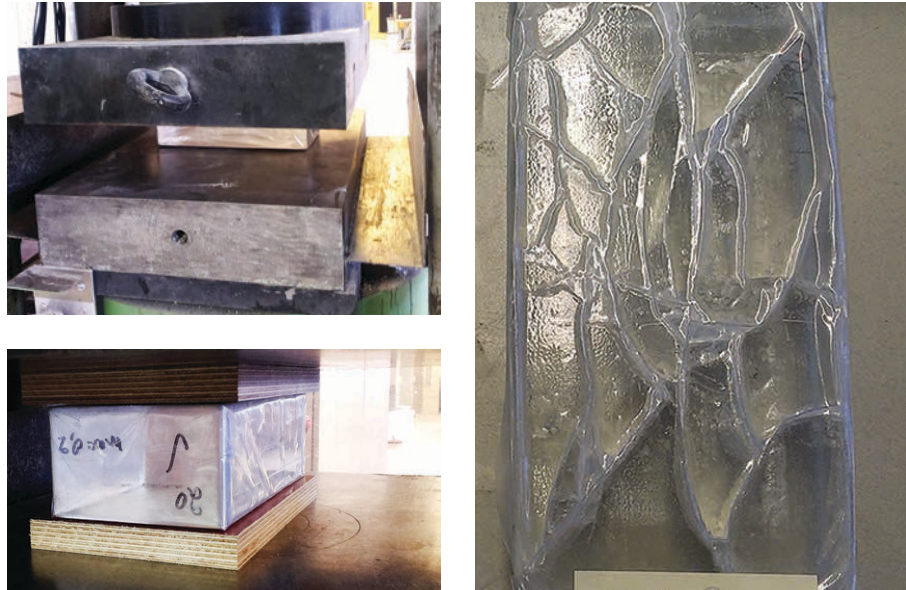
FIG. 5.22 Compression tests of glass blocks. Top left: Test set-up for the first two series. Bottom left: Test set-up for the specimens of the third series with plywood as intermediary. Right: Typical initial crack pattern in specimen.

5.6.2 Compressive tests on columns out of adhesively-bonded glass blocks

Table 5.6 gives an overview of the results of the compression tests on the 4 glass columns. All specimens were tested until complete failure, thus, the values mentioned at Table 5.6 concern the ultimate failure stress of each column. Essentially, at the stated stress values, the specimens lost their integrity, as cracks propagated through the blocks causing the entire assembly to split or shutter (Fig.5.24). Forking (branching) of the cracks was denser and greater as the applied stress increased: specimens B_{NS1} and B_{NS2} essentially shuttered into pieces compared to specimens B_{NL1} and B_{NL2}.

TABLE 5.6 Results of the compression tests on the glass column specimens

Specimen	Dimensions [mm]	Observations	Failure load [kN]	Nominal compressive stress at failure [MPa]
BNL1	232x106x492	Bonding across the large surfaces Inconsistent bond thickness, up to 0.5 mm thick in the middle	2090	85
BNL2	246x106x464		1296	49.7
BNS1	116x121x484	Bonding across the small surfaces Consistent, approx. 0.2-0.3 mm, bond thickness	1597	113.8
BNS2	116x121x484		1484	105.7

A crucial observation on the failure behaviour of the specimens is that the cracks, initiated at one of the glass blocks, did not follow the adhesive joints between the bricks, as would be anticipated in a conventional masonry assembly, but propagated through the glass elements as if it the assembly was one monolithic unit (see Fig.5.23). This indicates that in compressive stresses of the examined magnitude the applied adhesive has higher resistance to delamination than glass has to crack propagation.

Furthermore, the compression tests of the 4 glass columns revealed significant differences in the compressive strength of the different configurations. This can be attributed to:

— the creation of indirect local tensile stresses due to the oblong shape of the specimens
— the different configurations of the glass blocks
— improper bonding

Indeed, prototypes B_{NL1} and B_{NL2} that presented non-homogeneous bonding demonstrated down to half the strength than prototypes B_{NS1} and B_{NS2}. The latter specimens follow a different configuration and block size that allows for a constant and comparably thinner adhesive layer. Due to the stronger adhesive bonds formed, B_{NS1} and B_{NS2} columns showed a noticeably more monolithic behaviour and a higher compressive strength.

Although the number and size of the samples are limited for deriving quantitative results, they indicate that the compressive strength of the structure is greatly influenced by the quality of the bonding surfaces and thus, by the thickness of the adhesive layer.

FIG. 5.23 Left: B~NS~ column prior to testing. Centre left: Initiation of crack. Centre right: Same specimen at complete failure. Right: Intact piece of the tested specimen after failure: the principal crack essentially propagated vertically, defying the adhesive joints.

FIG. 5.24 The glass column specimens after testing. Left two pictures: B~NS~ specimens. Right two: B~NL~ specimens

5.6.3 4-point bending tests on adhesively bonded beams

In accordance with the failure load and geometry of each specimen, the nominal flexural strength formula was used in order to derive the flexural strength:

$$\sigma = \frac{3F(L\text{-}L_i)}{2bd^2}$$

EQUATION 5.1

Symbol	Definition	Unit	Experimental set-up value
σ	flexural strength	MPa	-
F	load at the fracture point	N	-
L	length of the outer (bottom) support span	mm	1000
Li	length of the inner (top) support span	mm	300
b	width	mm	210
d	height	mm	195

The results of the experimental testing are summarized in Table 5.7 below:

TABLE 5.7 4-point bending tests results

Specimen	Failure Load [N]	Nominal Flexural strength [MPa]	Failure zone	Failure mode
C_1	42800	5.63	One block offset from the middle	Vertical cut without branching, essentially splitting the beam in two halves
C_2	36400	4.79	middle	
C_3	38600	5.08	middle	
C_4	53300	7.01	middle	

The results of the 4-point bending tests suggest an in-plane flexural strength at failure between 4.79-7.01 MPa, with most specimens failing at a flexural stress value closer to 5 MPa. Hence, a flexural strength of 5 MPa can be used as a conservative design value, given the fact that the flexural strength of glass itself is considerably higher. The lower values in fact occur because the beam specimens are only bonded horizontally, resulting to stress concentrations on the open vertical joints, which decrease the strength of the specimen. Nonetheless, in the actual façade construction, the glass blocks are confined by the boundaries of the structure and therefore the vertical joints of the wall are prevented from opening, hence, the strength is expected to be higher. No visible cracks were observed before the specimens reached the failure load.

The fracture pattern of the specimens clearly demonstrates the monolithic behaviour of the adhesively bonded glass block assembly and the absence of considerable internal residual stresses: All specimens failed with a straight, parallel to the loading direction cut, following one of the top and bottom open vertical joints. In specific, specimen C_1 broke in an offset of one block from the middle, while the rest of the specimens failed at their middle. In all cases, the glass block of the middle horizontal layer corresponding to the propagating vertical joint was split in half. No significant

delamination nor branching of the crack was observed at any of the specimens. The breaking pattern indicates that the adhesive's shear strength is sufficient to assure that the beam specimens behave in a monolithic way under failure.

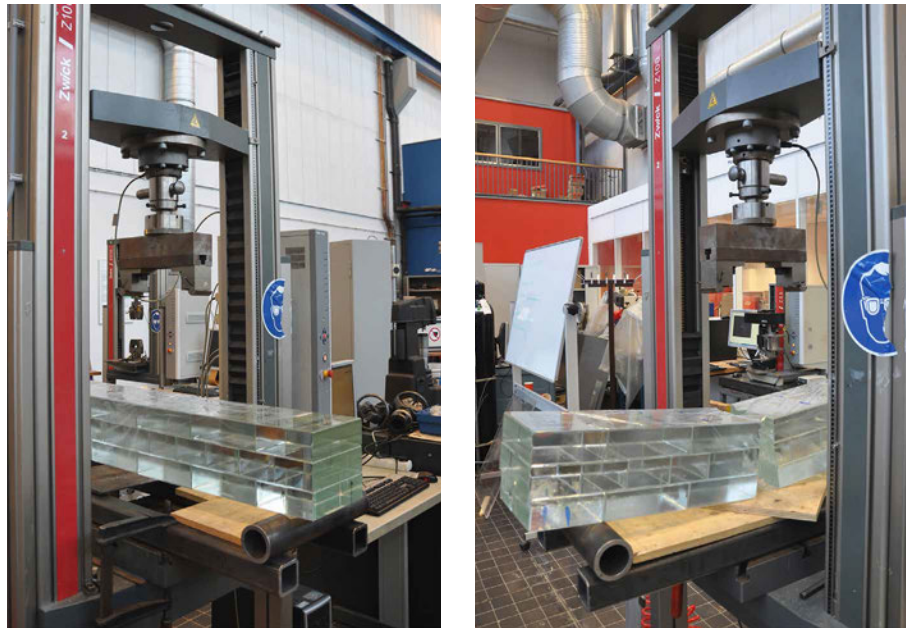The typical failure pattern of the specimens are seen in Fig. 5.25 and Fig. 5.26:

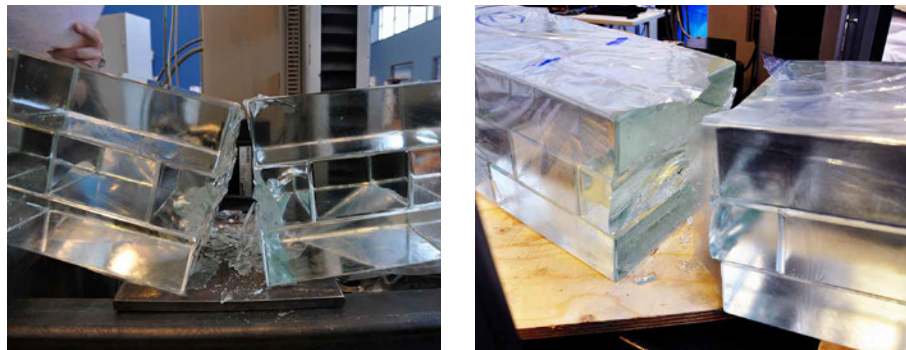FIG. 5.25 Left: Experimental set-up. Right: Typical failure mode (Specimen C_3)

FIG. 5.26 Typical failure mode of specimens, a clear, vertical cut at the middle of the beam.

4-point bending test on adhesively bonded glass architrave

Table 5.8 provides an overview of the geometrical characteristics and failure mode of the tested architrave.

TABLE 5.8 Results of the 4-point bending test of the architrave

Specimen geometric characteristics	Failure Load [N]	Nominal Flexural strength [MPa]	Failure zone	Failure mode
L = 1740 Li = 280 b=210 d=255[†] (average)	41600	6.7	Vertical joint where *DP 4494* was applied.	Vertical cut without branching, essentially splitting the specimen in two halves

[†] *The height of the specimen varies from 255-330 mm; however, the area where the height increased above 255 mm is constrained at a small zone close to the edges of the specimen. Thus, the height variation was neglected from the calculation under the assumption that the highest bending moments occur in the middle zone where the height is constantly 255 mm.*

Delo 4468
monolithic behavior: failure on glass

Delo 4494
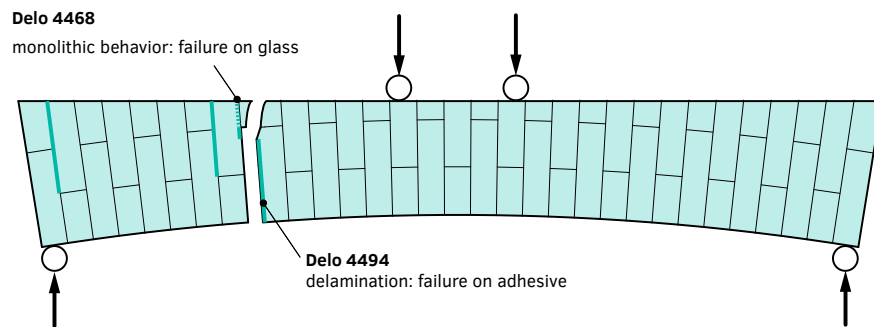delamination: failure on adhesive

FIG. 5.27 Illustration of the breaking pattern of the tested specimen

The arch specimen failed at 41600 N, corresponding to an approximate nominal flexural strength of 6.7 MPa. At that load the specimen split by a clear cut in 2 uneven pieces, as illustrated in Fig. 5.27. Prior to the failure load, no cracks were observed. In particular, the specimen instead of breaking in the middle zone where bending moments are the highest, as was the case with the beam specimens tested in 4-point bending, split at the closest to the centre joint where *DP 4494*[45]

---

45 *DP 4494* was applied due to a thicker joint that could not be sufficiently covered by *DP 4468*

was applied. In that location, the bottom block, which was bonded with *DP 4494*, delaminated, subsequently causing crack propagation. However, the crack path did not follow the upper seam, which was bonded with *DP 4468*, but instead, continued within the glass interface of the upper block as can be seen in Fig. 5.28. No visible delamination of the *DP 4468* adhesive was observed. Although this single experiment cannot be used for deriving quantitative data, it provided valuable input on the influence of different adhesives of the DP family on the failure behaviour and strength of the assembly. The experiment suggested that (1) a thicker joint and (2) the use of *DP 4494* can reduce or even alter the structural behaviour and capacity[46] of the assembly. Nonetheless, the tested architrave could withstand a substantial load, more than double[47] than the one anticipated by the structural engineers of the project.
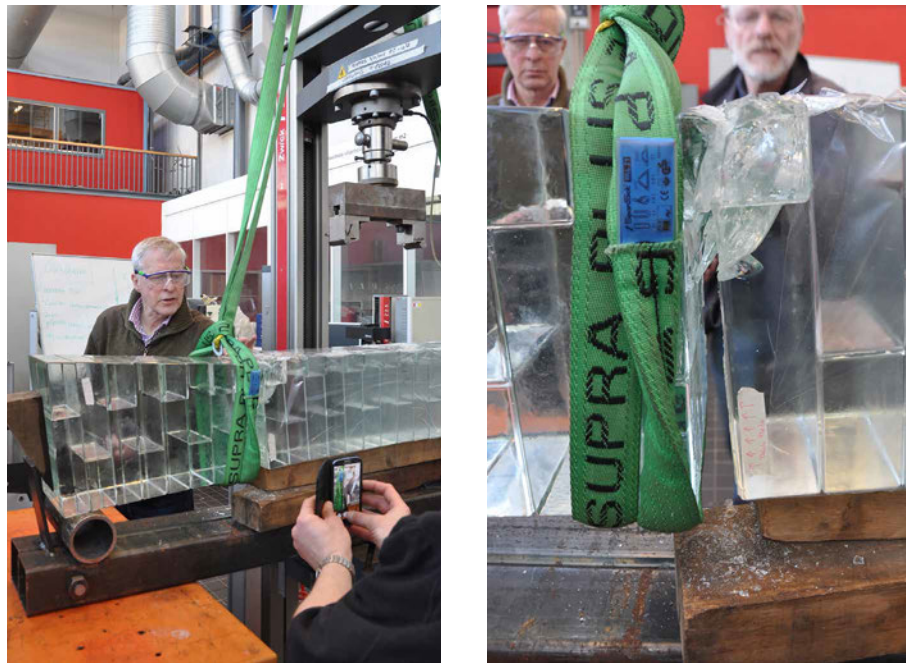

FIG. 5.28 The architrave specimen after failure.

---

46   Although in literature *DP 4494* presents higher values in both tensile strength and Young's Modulus, it is an adhesive engineered principally for plastic bonding. It presents good adhesion to glass but with a comparatively decreased mechanical performance than the one stated in literature.

47   According to the calculations by *ABT structural engineers*, the architrave specimen should be able to withstand 20 kN of load prior to failure.

5.6.5 Impact and vandalism test

Table 5.9 summarizes the findings from the hard-body impact and vandalism tests:

TABLE 5.9 Findings from the hard-body impact and vandalism test

Test	Test repetition	Observations
Hard-body impact test release from 45°	2	No damage on the glass specimen. Concrete suspended block chipped off at its corner
Hard-body impact test release from 90°	2	No damage on the glass specimen. Concrete suspended block chipped off at its corner
Vandalism test	2	Aimed block cracked mainly internally. No damage on the adjacent blocks. The same observations applied on the 2nd test, which was performed on one of the blocks adjacent to the cracked one.

The glass wall prototype resisted successfully all 4 impact tests without presenting any visible cracks; the concrete brick used as impactor was severely damaged. Accordingly, it is expected that the facade can withstand the accidental impact of normal objects such as bikes, bottles, etc.

The vandalism test with a sledgehammer resulted to internal cracks to the aimed glass block. No damage or crack propagation occurred to any of its adjacent blocks. A second, adjacent block was then hit by the sledgehammer, and the same internal cracking pattern appeared (see Fig. 5.29). The results indicate that (1) a rapid impact force only causes local damage, which does not transfer to adjacent bricks and (2) the damaged blocks still maintain a smooth external surface – there is no risk of passers by being hurt by flying shards. It should be noted that an unavoidable by-product of the glass facade is that the glass blocks will already be in compression due to the self-weight of the structure. Nonetheless, the anticipated pre-compression of the blocks is not expected to significantly alter the results[48].

The vandalism test emphasized the significance of developing a replacement method in case a brick is damaged. Accordingly, a procedure of replacing a damaged brick was developed using the same specimen:

---

[48] Considering the total dimensions of the façade and based on an even dead-load distribution the expected pre-compression of the entire envelope is of less than 0.2 MPa at the lower rows of the façade. Even if the entire weight of the façade (approx. 40 tn) is imposed uniformly on one of the S blocks, it would not result to more than 19 MPa of pre-compression.

First the largest part of the mass of the damaged block is mechanically removed until only small shards attached to the adhesive are left. The adhesive is then locally heated above 120 °C with a hot air blower. This is the transition temperature where *DP 4468* starts to become viscoelastic and softer, allowing for easy mechanical removal of the last glass shards and of the adhesive layer itself, without damaging the adjacent blocks. A new glass block, machined down by 0.1 mm in dimensions to slide easily into the empty slot, can be then inserted (see Fig. 5.29, bottom right). Adhesive can then be injected into the surrounding seams, using a syringe.

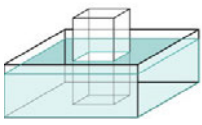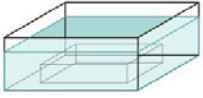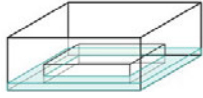FIG. 5.29 Top: Result of the first vandalism test. Bottom left: Following, the vandalism test was repeated to an adjustent brick. Again, only the aimed block was damaged. Bottom right: The prototype after the replacement of one of the damaged blocks.

Thermal shock tests on individual blocks

The results of the thermal shock tests are summarized in Table 5.10.

TABLE 5.10 Results of thermal shock tests. Two samples were used per test per temperature.

T.	F_1	F_2	F_3	F_4
60°C	Interior cracks only at the part that was in the water.	Completely cracked in the interior.	No cracks	No cracks
80°C	Interior cracks only at the part that was in the water. The cracks are more severe than in 60 °C.	Completely cracked in the interior. The cracks are more severe than in 60 °C.	No cracks	No cracks

Specimens F_3 and F_4 are the closest simulation of the hot facade's resistance against summer rain; in the event of rain, only the external surface of the blocks will be exposed to rainwater. No cracks appeared in either case. However, all specimens from the F_1 and F_2 series that were half- or completely immersed into water after being heated to 60°C or 80°C presented considerable cracks in their interior due to the abrupt temperature change between their surface and the core. More specifically, both F_2 samples developed internal cracks throughout their volume, while in specimens of the F_1 series cracks were observed only in the part that was immersed in water (see Fig. 5.30). In that case, a clear, almost horizontal cut marks the waterline. In all samples of the F_1 and F_2 series, the cracks continued to grow significantly after they were removed from the water (Fig. 5.30).

The results suggest that the blocks can withstand the elements if applied in an external building wall such as the case study, where they will be susceptible to a rapid temperature change mainly on their external surface. Nonetheless, the blocks may be susceptible to damage in locations with extreme weather conditions. If the concept is to be used in a less moderate climate than Amsterdam, it is recommended to test for thermal shock using appropriate parameters and/or consider the use of borosilicate glass that has a significantly improved thermal shock resistance.

FIG. 5.30 Specimens of the F$_1$ and F$_2$ series tested in thermal shock from 80 °C to 20 °C. Left: Cracks in the specimens immidiately after they were removed from the water. Right: Growth of the cracks in the same specimens after approx. one day.

5.7 Conclusions

An innovative, self-supporting glass masonry wall system, consisting of annealed soda-lime solid glass blocks bonded together by *Delo Photobond 4468*, a UV-curing, colourless adhesive has been developed for the *Crystal Houses* façade in Amsterdam.

The conducted experimental work proves the structural feasibility of the given case study: the structural system developed for the *Crystal Houses* façade allows for a glass wall of considerable dimensions that can carry its own weight without cracking or buckling. In fact, even one glass block can successfully carry the entire weight of the façade if properly supported. In particular, the experimental results indicate that the structure presents a monolithic behaviour against the anticipated load, offering compressive and flexural strength comparable to or better than the strength of typical B80 high performance concrete.

The flat geometry of the facade and its high slenderness ratio necessitate the reinforcement of the facade against lateral forces and buckling that may occur due to eccentricity in construction, or wind. This is done by the four 5.5 m tall buttresses on the inner side of the glass wall. In this way a completely transparent solution is achieved using the geometry of the facade, sparing the necessity of additional non-transparent steel elements.

Visual prototypes and structural experiments demonstrated that the glass components' dimensional tolerances should not exceed ±0.25 mm deviation in size

and flatness. Visual prototypes with a larger deviation in the height and flatness of the glass blocks could not be homogeneously bonded, resulting in visible air gaps and dendritic patterns in the adhesive layer. Furthermore, inhomogeneous bonding can significantly reduce the structural performance of the assembly, as was proven by the compression tests on adhesively bonded glass columns and by the 4-point bending test of the architrave specimen. Among the column specimens tested in compression, the prototypes with improper bonding failed at considerably lower stress values than the specimens made of glass blocks of stricter dimensional and surface tolerances, ensuring a consistent and comparably thinner adhesive layer. The architrave testing further confirmed the importance of proper bonding and of the use of *DP 4468* as the bonding media: The architrave specimen failed in the closest to the centre location where another adhesive, *DP 4494*, was applied due to a considerably larger gap that could not be filled with *DP 4468*. The specimen delaminated where *DP 4494* was used, whereas on the upper layer, which was bonded with *DP 4494*, a crack was initiated within the glass.

The beam specimens tested in 4-point bending, which were made of blocks of the recommended ±0.25 mm tolerance presented a consistent, monolithic failure of the assembly and indicated a flexural strength of the system of approx. 5 MPa. The failure mechanism of the glass-adhesive assembly is different than the one of conventional masonry works, where the cracks follow in principle the mortar joints.

Compression tests on single blocks emphasized the importance of a proper connection design: Glass blocks directly in contact with the steel surface of the testing machine failed at values between 20-30 MPa, whereas blocks that were tested with plywood as intermediary reached the load limit of the machine without failure; essentially, each block could withstand more than the entire load of the façade.

All the above emphasize the importance of strict tolerance specifications in the brick fabrication and the necessity of a homogeneous adhesive layer of the recommended thickness in order to ensure a consistent, predictable and optimum structural and visual performance.

The impact and vandalism tests demonstrate that the *Crystal Houses* façade can withstand accidental impacts of objects but may endure cracks in case of vandalism. This stresses the necessity of a replacement method in case of a damaged element. Accordingly, a replacement method by controlled heating of the adhesive has been developed and experimentally proved.

Given the high dimensional precision required for the cast units, soda-lime glass and open moulds were preferred to reduce the manufacturing costs, as the post-processing of the elements was considered inevitable. Even though in soda-lime glass the thermal stresses occurring are much higher than for borosilicate glass, the experiments prove that soda-lime glass blocks can withstand the anticipated rapid temperature changes when applied to an external wall in a temperate climate.

Overall, although the experiments and research presented were conducted for the specific case study, the principles and experimental data of the adhesively bonded solid glass block system can be used as an established guideline for further structural or self-supporting applications of the developed adhesively bonded system.
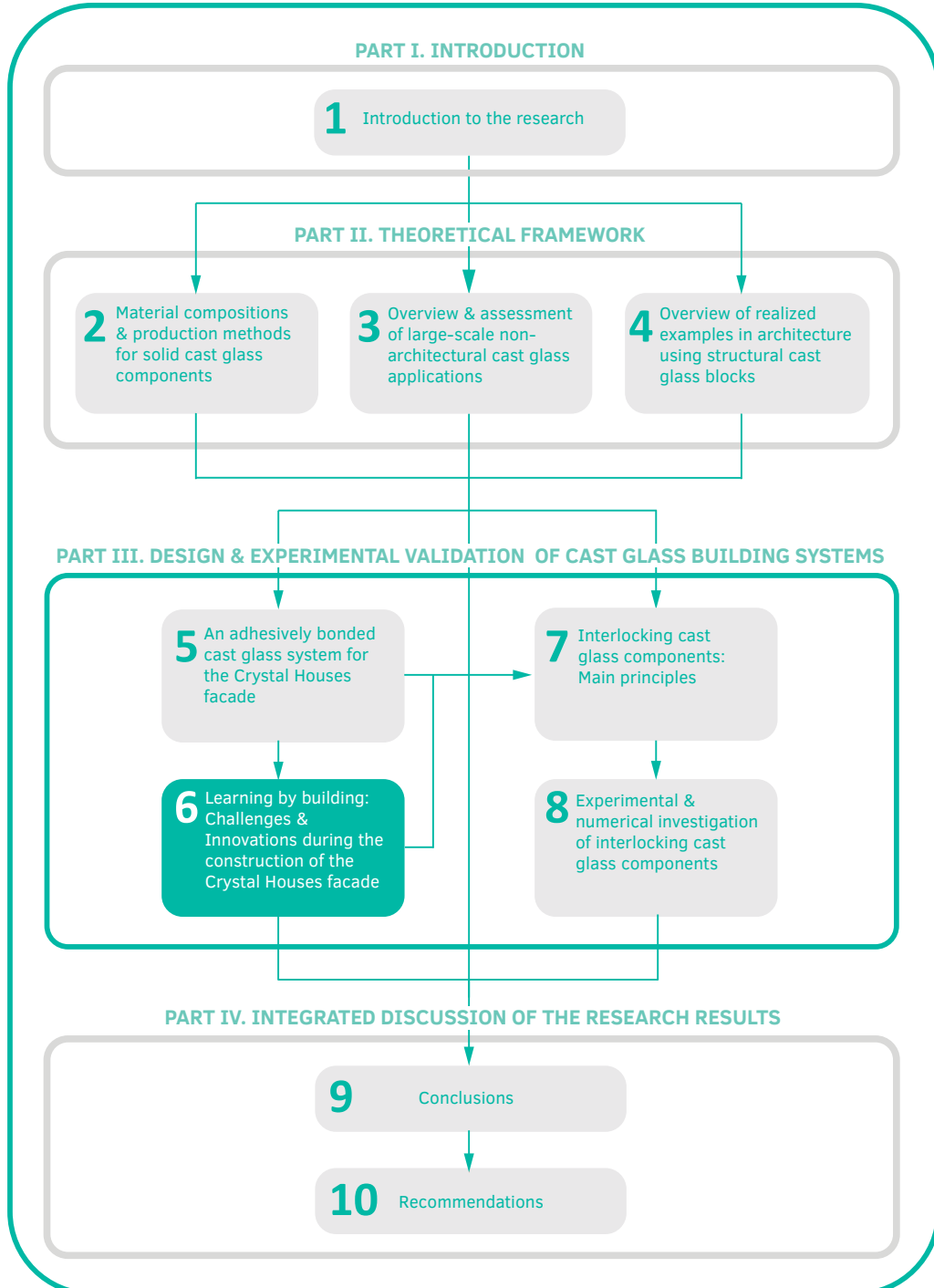
The *Crystal Houses* facade

Exploring the third dimension of glass

PART I. INTRODUCTION

1 Introduction to the research

PART II. THEORETICAL FRAMEWORK

2 Material compositions & production methods for solid cast glass components

3 Overview & assessment of large-scale non-architectural cast glass applications

4 Overview of realized examples in architecture using structural cast glass blocks

PART III. DESIGN & EXPERIMENTAL VALIDATION OF CAST GLASS BUILDING SYSTEMS

5 An adhesively bonded cast glass system for the Crystal Houses facade

7 Interlocking cast glass components: Main principles

6 Learning by building: Challenges & Innovations during the construction of the Crystal Houses facade

8 Experimental & numerical investigation of interlocking cast glass components

PART IV. INTEGRATED DISCUSSION OF THE RESEARCH RESULTS

9 Conclusions

10 Recommendations

Solid cast glass components and assemblies for structural applications

TOC